

Sustainable Hydrogenation of Nitroarenes to Anilines with Highly Active *in-situ* Generated Copper Nanoparticles

F. Pelin Kinik^[a], Tu N. Nguyen^[a], Mounir Mensi^[b], Christopher P. Ireland^[a],
Kyriakos C. Stylianou*^[a] and Berend Smit*^[a]

[a] Laboratory for Molecular Simulation (LSMO), Institute of Chemical Sciences and Engineering (ISIC), École Polytechnique Fédérale de Lausanne, CH-1950 Sion, Switzerland.

[b] Institute of Chemical Sciences and Engineering (ISIC), École Polytechnique Fédérale de Lausanne, CH-1950 Sion, Switzerland.

e-mail: kyriakos.stylianou@epfl.ch and berend.smit@epfl.ch.

Abstract: Metal nanoparticles (NPs) are usually stabilized by a capping agent, a surfactant, or a support material, to maintain their integrity. However, these strategies can impact their intrinsic catalytic activity. Here, we demonstrate that the *in-situ* formation of copper NPs (Cu⁰NPs) upon the reduction of the earth-abundant Jacquesdietrichite mineral with ammonia borane (NH₃BH₃, AB) can provide an alternative solution for stability issues. During the formation of Cu⁰NPs, hydrogen gas is released from AB, and utilized for the reduction of nitroarenes to their corresponding anilines, at room temperature and under ambient pressure. After the nitroarene-to-aniline conversion is completed, regeneration of the mineral occurs upon the exposure of Cu⁰NPs to air. Thus, the hydrogenation reaction can be performed multiple times without the loss of the Cu⁰NPs' activity. As a proof-of-concept, the hydrogenation of drug molecules “flutamide” and “nimesulide” was also performed and isolated their corresponding amino-compounds in high selectivity and yield.

Introduction

Recent advances in our understanding of heterogeneous catalysis is that, although a catalyst keeps its stoichiometry, it can change shape, size and structure during the reaction.^[1] In fact, one can argue that the most active catalysts can exhibit variety of structural alterations during reactions due to their high surface energy, leading to a lower energy of the transition state and hence higher reaction rate.^[2] Therefore, it can be deduced that the most active catalysts encounter with the instability problems more frequently.^[2] Copper nanoparticles (Cu⁰NPs) are

reported to be among the most active catalysts for a wide range of catalytic reactions, including water-gas shift,^[3] hydrogenations,^[4] organic transformations such as cycloaddition^[5] and cross coupling,^[6] as well as photocatalytic reactions.^[7] Despite the versatility of catalytic reactions with Cu⁰NPs, their low stability has been a great challenge, and this is the critical drawback for industrial applications.^[8]

Cu⁰NPs can be deactivated due to many different mechanisms, such as sintering and aggregation, oxidation, deposition of reactants or products covering the surface, or poisoning of the catalyst. Many strategies have been developed to stabilize Cu⁰NPs such as the employment of capping agents (e.g., polymers and surfactants)^[9] and supports (e.g., oxides, polymers and zeolites)^[10] or the generation of core-shell structures with other metals (e.g., Ag, Ni, and Pd).^[11] These strategies, however, often only address one of the issues mentioned above and they are short term solutions. For example, using capping agents can effectively prevent the aggregation of Cu⁰NPs; however, they can also act as a “poison” and limit the accessibility of reactants to the catalytically active sites. Moreover, they can be detached from the NPs under some reaction conditions, which might have a detrimental effect on the stability of Cu⁰NPs over several catalytic cycles.^[12] In case of using supporting matrices, obtaining a uniform distribution of the Cu⁰NPs is challenging, and the aggregation of NPs might still occur before or during the catalytic cycles.^[10] Similarly, creating core-shell structures of Cu⁰NPs with other metals might not prevent the catalytic deactivation.^[13] Therefore, a fundamentally different strategy is needed to address the stability challenges that Cu⁰NP catalysts encounter. Our strategy is based on the notion that any attempt to stabilize Cu⁰NP catalysts may change their intrinsic catalytic activity. We therefore explore an approach, in which we aim to develop materials that generate these nanoparticles *in-situ*.

Recently, we have shown that the synthetic form of the Jacquesdietrichite mineral with the chemical formula of (Cu₂[(BO)(OH)₂](OH)₃)^[14] generates Cu⁰NPs *in-situ* as an integral part of the hydrolytic dehydrogenation of ammonia borane (AB).^[15] AB can be considered as an alternative high quality H₂ source since it possesses a high H content of 19.6 wt% and is robust, non-toxic and highly soluble in aqueous solutions. By the hydrolysis of AB, hydrogen release occurs at room temperature and under ambient pressure, eliminating the safety issues and the poor solubility problem of H₂ gas in water.^[16] We demonstrated that after the hydrogen generation from AB is complete, fresh and highly crystalline mineral microcrystals are regenerated from Cu⁰NPs in a quantitative yield. Therefore, AB hydrolysis was performed for at least 10 cycles with negligible decrease of the catalyst’s activity. This result is inspiring since the fresh Cu⁰NPs can be generated from the synthetic mineral when needed, preventing them

from aggregation, oxidation, and deposition. This is an attractive strategy of limiting the deactivation problems of Cu⁰NPs and the difficulty in their handling and storage.

In this work, we show that our strategy can be generalized to the hydrogenation of nitrobenzenes to anilines, by utilizing the hydrogen generated from AB and using the *in-situ* generated Cu⁰NPs. Anilines are key intermediates in the production of dyes, pharmaceuticals, and fragrances. In industry, the hydrogenation of nitrobenzene to aniline is conducted in the gas phase with copper or nickel catalysts at high temperatures of 553–573 K and pressures of H₂ of 0.1–0.5 MPa.^[17] However, in some cases of nitroarene reduction under the conditions used in industry, Cu catalysts are exposed to a comparatively fast deactivation, and reactivation is required.^[18] In the literature, other noble and non-noble metal nanoparticles have been also investigated for the hydrogenation of nitroarene compounds. Since copper is an earth-abundant and one of the cheapest non-noble metals, Cu⁰NPs have been an attractive alternative for this catalytic process. In our study, we propose a strategy to protect Cu⁰NPs during the hydrogenation of nitrobenzenes to their corresponding anilines from the most common catalyst deactivation problems such as agglomeration and oxidation, without using any other metal, capping agent or support material.

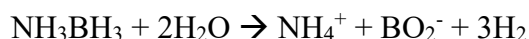
Of particular interest of the nitro compounds are two drug molecules, flutamide (a nonsteroidal antiandrogen drug which is used primarily to treat prostate cancer)^[19] and nimesulide (a nonsteroidal anti-inflammatory drug for pain medication and fever reducing),^[20a] where the hydrogenation can be carried out to make these drug molecules more compatible with the body.^[20] For the hydrogenation of these molecules, Jagadeesh et al.^[21] developed an earth-abundant catalyst, Fe₂O₃, which performs the reaction at 120 °C with a hydrogen pressure of 50 bar in 15 hours. In pharmaceutical industry, hydrogen gas is often used with a flammable organic solvent, which increases the safety risk within the manufacturing facility. Moreover, H₂ gas has a limited solubility in solvents (especially in water) and therefore there is a need for high pressure for the utilization in hydrogenation reactions.^[22] Therefore, one would expect that the introduction of highly active Cu⁰NPs, and the use of AB as the hydrogen source, would allow these reactions to be performed at milder conditions efficiently.

Herein, we present that the *in-situ* generation of Cu⁰NPs from the synthetic mineral in the presence of AB was successfully used to catalyze the reduction of nitroarene compounds to their corresponding anilines by utilizing the hydrogen generated from AB, with good selectivity and yields. The catalytic activity and the integrity of the Cu⁰NPs remained almost unaffected for at least 5 cycles of reaction, which is due to the reformation of fresh mineral at the end of each cycle. The reusability of the mineral for the generation of fresh Cu⁰NPs in each

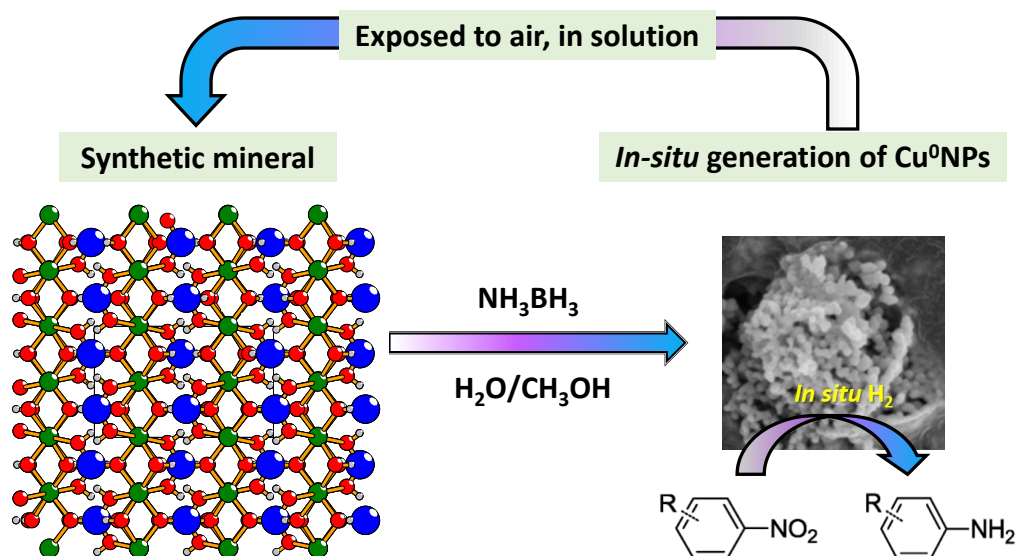
cycle prevents the catalyst poisoning and the use of stabilizing agents. The efficient reduction of a wide range of nitro substrates, including drug molecules flutamide and nimesulide, illustrates the versatility of our strategy.

Results and Discussion

Our strategy of *in-situ* generation of Cu⁰NPs is illustrated in [Scheme 1](#). The synthetic mineral generates Cu⁰NPs in water in the presence of a reduction agent, ammonia borane (AB), which is the source for hydrogen. The hydrolytic dehydrogenation of AB is catalyzed by *in-situ* generated Cu⁰NPs and hydrogen is released into the reaction solution. The solution also contains the reactants for the hydrogenation reaction, and the conversion of nitroarene to aniline takes place in parallel using the in-situ generated hydrogen from AB. In our study, the formation of by-products arising from ammonia borane hydrolysis was not investigated since the unravelling of the reaction mechanism as well as process optimization and design (e.g., regeneration of spent ammonia borane) is hindered. The composition of B-containing by-products is controversial, which could be attributed to different assignments of ¹¹B NMR and/or FTIR spectra for the B-containing by-products.^[23] Since undesired by-products such as borazine (B₃N₃H₆) can be liberated in the case of thermolysis of ammonia borane, hydrolysis of ammonia borane was performed for the release of hydrogen:



As we interpreted in our previous study,^[15] the re-formation of synthetic mineral (Cu₂[(BO)(OH)₂](OH)₃) at the end of each hydrogenation cycle can be attributed to the oxidation of the in-situ generated Cu⁰NPs by their exposure to air, in combination with the presence of BO₂⁻ ions, which is the product resulting from the hydrolysis of ammonia borane in the reaction mixture. Therefore, the accumulation of BO₂⁻ ions in the reaction solution over repeated cycles can be eliminated. Since the material is regenerated in the pure and fresh form, the generation of new and active Cu⁰NPs can catalyze the hydrogenation reaction without any loss of their catalytic activity.



Scheme 1. Schematic illustration of *in-situ* generation of Cu⁰NPs from the synthetic mineral using ammonia borane (AB) as the reducing agent, with the simultaneous conversion of nitroarenes to anilines by *in-situ* hydrogenation. Fresh mineral can be regenerated at the end of the reaction upon the exposure of reaction solution to air, resulting in the formation of fresh Cu⁰NPs for the next cycle. Color code for mineral: oxygen in red, copper in green, boron in blue.

The as-synthesized synthetic mineral and *in-situ* generated Cu⁰NPs were characterized by powder X-ray diffraction (PXRD) (Figure 1a and 1c), showing that the experimental PXRD patterns of both materials matched well with the simulated ones. The SEM and TEM images obtained before and after the reaction confirm the formation of Cu⁰NPs, as our synthetic mineral consists of cuboid shaped single crystals (Figure 1b and S1a) while Cu⁰NPs with a size ranging between 20-40 nm are the only present compound after the reaction is complete (Figure 1d and S1b). The X-ray photoelectron spectroscopy (XPS) data was collected on as-synthesized mineral and *in-situ* generated Cu⁰NPs after the hydrogenation reaction (Figure 1e and 1f). Cu 2p XPS spectrum revealed that the synthetic mineral consisted of mostly Cu^{II} ($\geq 95\%$) ions. The XPS spectrum of *in-situ* generated Cu⁰NPs shows two components with binding energies at 932.5 and 934.5 eV corresponding to the Cu 2p_{3/2} core level, which can be assigned to Cu(0) and/or Cu(I) (932.5 eV), and Cu(II) (934.5 eV), respectively.^[24] Further information about the valence states of copper were obtained by analyzing the Cu LMM Auger spectrum of *in-situ* generated Cu⁰NPs obtained from XPS analysis (Figure S2). LMM spectra shows the presence of both, Cu(II) and/or Cu(I), as well as Cu(0). Together with the Cu 2p data analysis, it is

therefore clear that Cu(0) and Cu(II) are present. It is finally not possible to exclude Cu(I). In order to give more clarity to the findings of XPS, Auger electron spectroscopy was performed on the sample (Figure S3). The findings from both XPS and Auger electron microscopy analyses are in agreement with the PXRD pattern of the bulk material, showing that the majority of the sample consists of Cu(0). The observation of Cu(I) and Cu(II) is expected because of the surface oxidation of Cu⁰NPs due to the exposure of sample to air during the sample preparation.

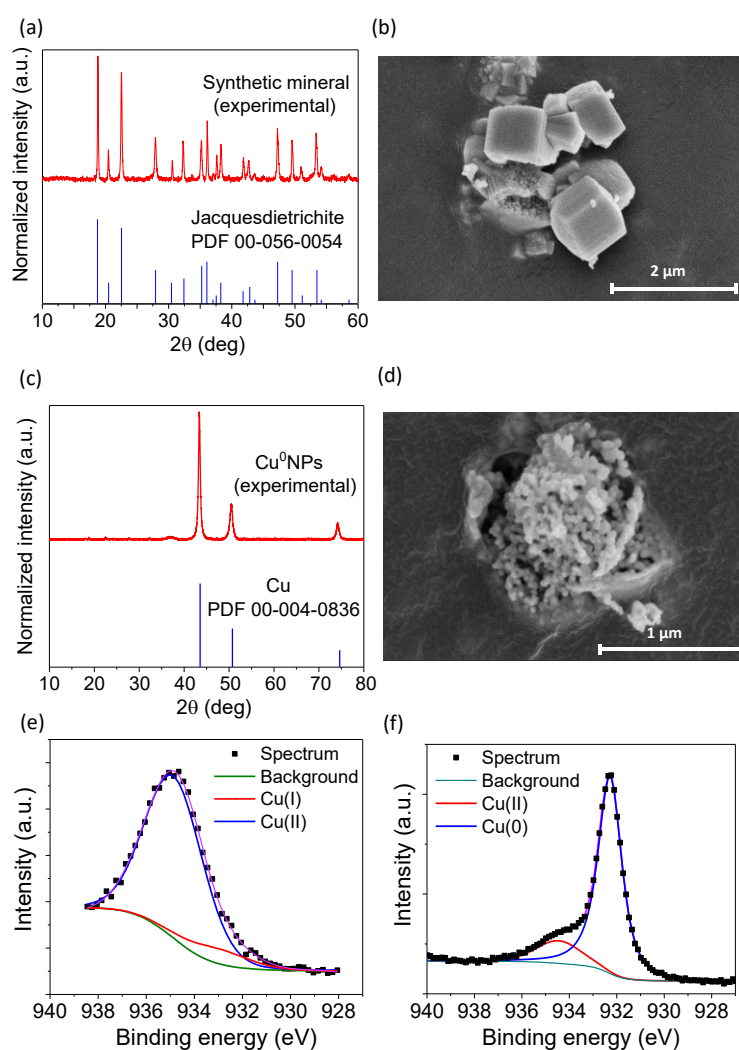
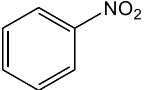
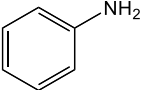
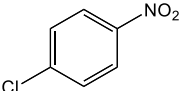
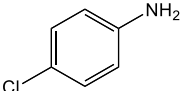
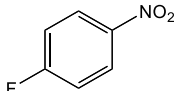
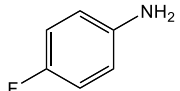
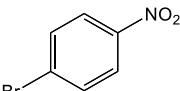
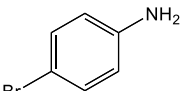
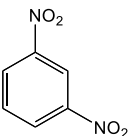
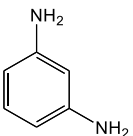
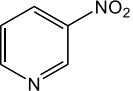
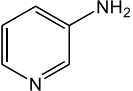


Figure 1. (a) Comparison of the simulated PXRD pattern of Jacquesdietrichite with the experimental PXRD pattern of our synthetic mineral. (b) SEM image of our synthetic mineral. (c) Comparison of the simulated PXRD pattern of Cu⁰NPs, with the PXRD pattern of *in-situ* generated Cu⁰NPs collected after the hydrogenation reaction. (d) SEM image of *in-situ* generated Cu⁰NPs collected after the hydrogenation reaction. Cu 2p XPS spectra of (e) as-synthesized mineral, (f) *in-situ* generated Cu⁰NPs.

To demonstrate the applicability of our strategy in hydrogenation reactions, we first investigated the catalytic activity of Cu⁰NPs toward the reduction of different nitroarenes as shown in Table 1. These nitroarenes represent different classes and each of these classes is used for the production of different intermediates. The simplest reaction is the reduction of nitrobenzene to aniline (Table 1, entry 1). The halogenated anilines (Table 1, entries 2, 3 and 4) are commonly used intermediates in the manufacture of herbicides, drugs and laboratory reagents^[25] and m-phenylenediamine (Table 1, entry 5) is used in the manufacture of azo dyes.^[26] 3-aminopyridine is an important building blocks in pharmaceuticals and agrochemicals (Table 1, entry 6).^[27] All reactions were carried out at room temperature using the optimized conditions (Figure S4). After combining all constituents of the reaction, the solution was sampled after 1 or 2 hours depending on the completion of the reaction. The yield and the selectivity of the products were determined by UV-Vis spectroscopy (Figure S5-10) and ¹H NMR analysis (Figure S11-16). In the absence of the catalyst, no conversion was observed. As shown in Table 1, except from 1-bromo-4-nitrobenzene and 3-nitropyridine, all investigated nitroarene compounds were converted within 1 hour with >90% yield and >99% selectivity. For 3-nitropyridine, we achieved a similar yield at the end of 2 hours while for 1-bromo-4-nitrobenzene, we obtained 40% yield after 2 hours also with 100% selectivity. The presence of the electron-withdrawing F- and Cl- groups does not affect the reaction and the aniline products were obtained in quantitative yields (Table 1, entries 2-3). In case of Br- analogue (Table 1, entry 4), the yield is 40%, which might probably be due to the lower electronegativity of Br compared to F and Cl; therefore, the nitro group is less electron deficient. The reduction of the nitro group is not affected by the presence of another nitro group, as shown for the case of 1,3-dinitrobenzene. In fact, both nitro groups were efficiently reduced to amines with 100% yield. Dell'Anna et al.^[28] reported similar findings, where the hydrogenation rate of 1-bromo-4-nitrobenzene is slower (61% yield in 6 hours) than that of 1,3-dinitrobenzene (96% yield in 6 hours). In that study, mono-amino products were observed only in negligible quantities during the reaction. Similarly, in our case, no mono-amino product was observed at the end of 1-hour reaction as indicated by NMR analysis. Therefore, it can be interpreted that the reduction of the intermediate product is fast, whereas electronegativity difference makes the reaction rate slower in the case of 1-bromo-4-nitrobenzene.

Table 1. Hydrogenation of various nitroarenes to anilines by the simultaneous *in-situ* formation of Cu⁰NPs and dehydrogenation of NH₃BH₃.

Entry	Substrate	Product	Yield (%)	Selectivity (%)	Time
1			>90	>99	<1 h
2			>99	>99	<1 h
3			>99	>99	<1 h
4			~40	>99	<2 h
5			>99	>99	<1 h
6			~83 (100)	>99	<1 h (<2 h)

Reaction conditions: 0.1 mmol nitro compound, 0.583 mmol AB, 12 mg catalyst, 1 ml MeOH, 9 ml H₂O, 25 °C.

As the stability and recyclability of the catalyst are highly crucial for practical applications, the integrity and catalytic performance of *in-situ* generated Cu⁰NPs were investigated. [Figure 2](#) shows the recyclability of the catalyst during five consecutive runs. Within the accuracy of UV-Vis instrument, aniline yield higher than 90% for each of the runs was observed without any catalyst deactivation ([Figure 2\(a\)](#)). As shown in [Figure 2\(b\)](#), there is no significant change in the PXRD pattern of the regenerated synthetic mineral after each reaction cycle, which indicates that the original synthetic mineral is fully recovered. Hence, each of the catalytic cycle is carried out with a fresh material and no loss of catalytic activity is observed. This finding is highly important since Cu-based catalysts might gradually lose their initial catalytic activity during the hydrogenation reaction, even when they are combined with

other metals or on supported porous media (Table S1). For example, Yu et al.^[29] prepared as-synthesized CuNi NPs and t-butylamine-treated CuNi NPs supported on graphene for the hydrogenation of aromatic nitro compounds by the methanolysis of AB. As-synthesized CuNi NPs could retain less than 40% of their initial activity at the end of the 5th cycle, and even after the treatment with t-butylamine and use of graphene as the support, the catalytic activity decreased to the 80% of the initial activity at the end of the 10th cycle, which is due to the weakened interaction between graphene and NPs through the cycles. In another example, Madasu et al.^[30] prepared polyhedral Cu crystals from Cu₂O cubes by using AB as the reducing agent, then performed simultaneous nitroarene hydrogenation at 30 °C. The hydrogenation of 4-nitroaniline to benzene-1,4-diamine was obtained with 100% conversion in the 1st cycle, but 88% conversion was observed for the 2nd cycle due to the catalyst deactivation.

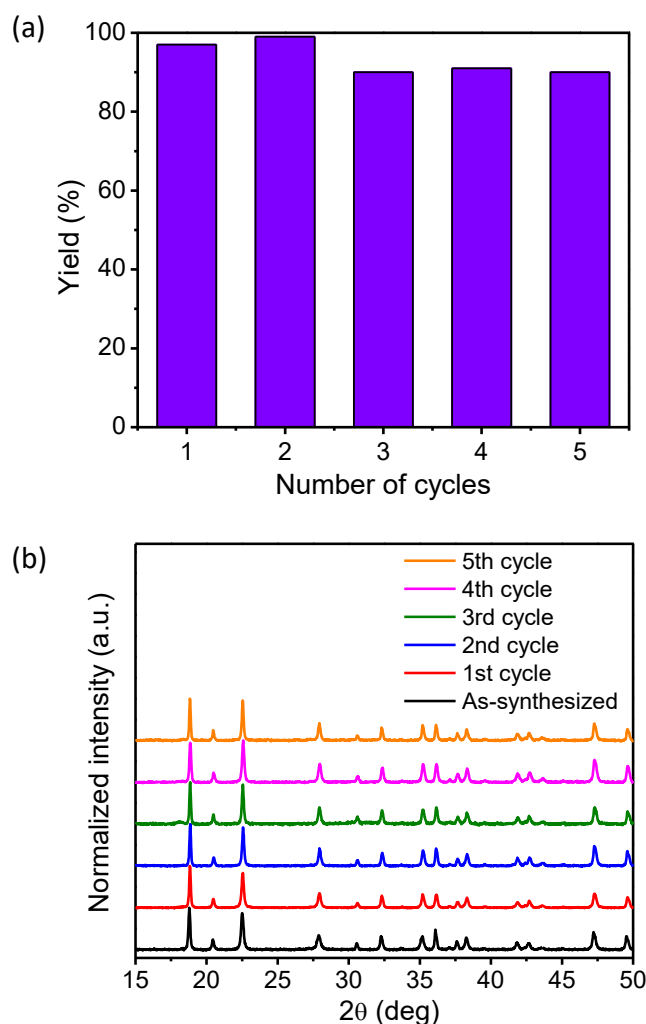


Figure 2. (a) Recycling experiments for the hydrogenation of nitrobenzene to aniline, showing the stability of the hydrogenation performance, (b) PXRD patterns of regenerated synthetic mineral at the end of each reaction cycle.

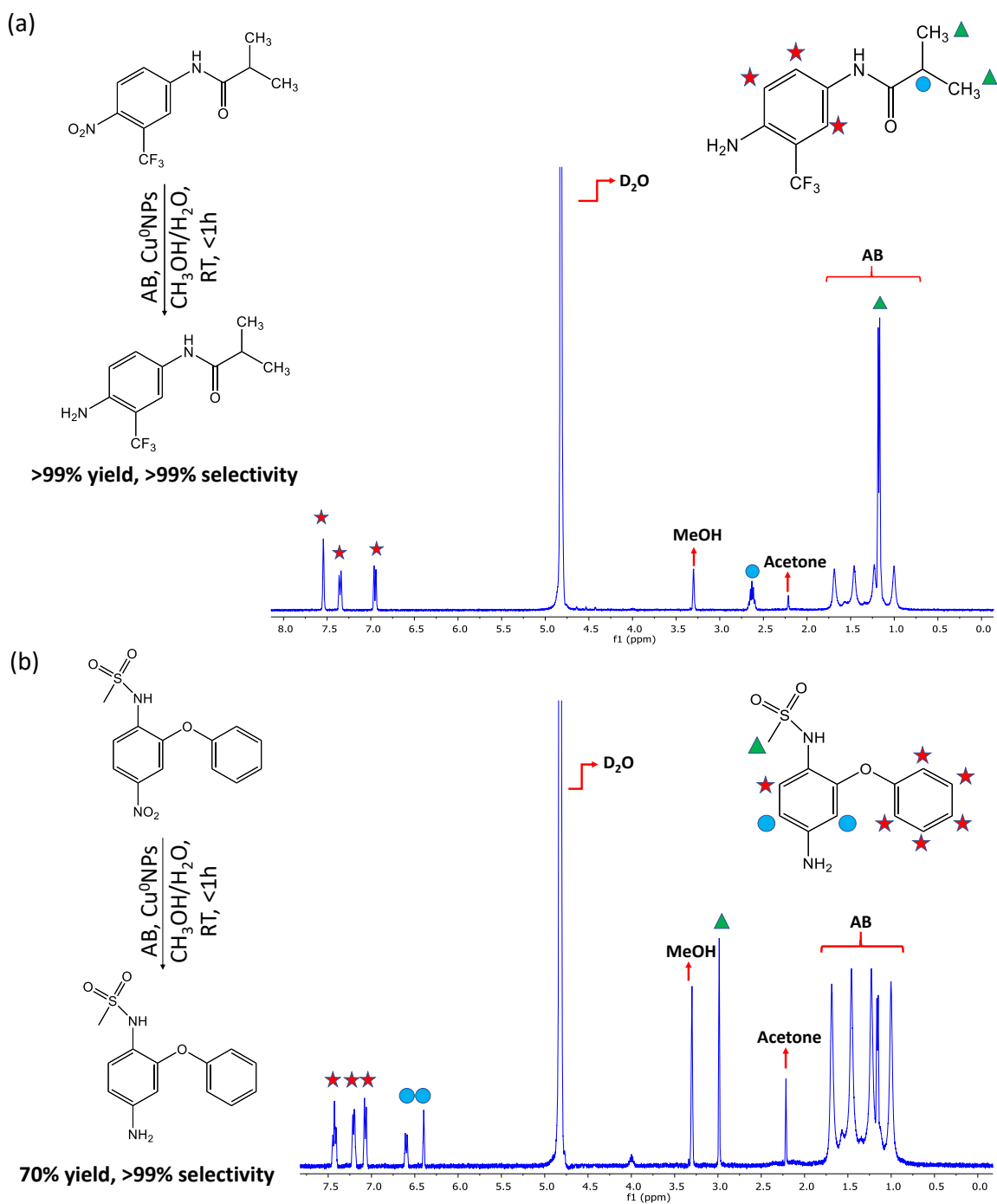


Figure 3. (a) Hydrogenation of flutamide and the confirmation of the purity of hydrogenated product by ^1H NMR analysis with the assignment of the peaks. (b) Hydrogenation of nimesulide and the confirmation of the purity of hydrogenated product by ^1H NMR analysis with the assignment of the peaks. Acetone is an impurity in both cases, arising from the cleaning of the NMR tubes. The reactions were performed for 1 hour in a mixture of deuterated methanol and deuterated water ($V_{\text{MeOH-d}_4}:V_{\text{D}_2\text{O}} = 1:9$) at room temperature.

The hydrogenation of drug molecules, flutamide and nimesulide, was studied using the same methodology as for the other nitroarenes to generalize our concept with different molecules. The only difference is that deuterated methanol and deuterated water were used to facilitate the determination of the purity, yield, and selectivity by ^1H NMR analysis (Figure S17-20, Supplementary Information). The yields of the reduced drugs were determined by ^1H NMR analysis, using tetrahydrofuran (THF) at a known concentration as the internal standard (Figure S19-20) Figure 3 shows that the catalytic performance of Cu^0NPs is outstanding; >99% selectivity toward the hydrogenation of $-\text{NO}_2$ to $-\text{NH}_2$ with high yield was observed, at room temperature, within 1 hour and ambient pressure. The reduction of nitro groups to their corresponding amines is challenging when other reducible groups (such as carbonyl, aldehyde, or alkene) are present in the structure. Moreover, the reduction of aromatic nitro compounds tends to stop at an intermediate stage, resulting in hydroxylamines, hydrazines and azoarenes.^[31] Although there are functional groups in drug molecules (e.g. carbonyl group in flutamide) that can also be reduced with H_2 , only the $-\text{NO}_2$ to $-\text{NH}_2$ hydrogenation was observed, without the formation of any intermediate product. The ^1H NMR spectrum (Figure 3a) shows that after the hydrogenation of flutamide, all chemical shifts are assigned to the corresponding amino-derivative compound, as there is not an additional doublet peak appearing, which proves the highly selective catalytic activity of *in-situ* generated Cu^0NPs . Moreover, for the reductions of both drug molecules, pure and fresh synthetic mineral could be recovered at the end of the cycle, and therefore no loss in catalytic activity is observed. One therefore would expect that the introduction of active Cu^0NPs , and the use of AB as the hydrogen source, would allow the hydrogenation reactions in pharmaceuticals to be performed at safer conditions (at room temperature and under ambient pressure) efficiently.

Conclusion

In summary, the *in-situ* generation of Cu^0NPs from the synthetic Jacquesdietrichite mineral was successfully applied for the reduction of nitroarene compounds to their corresponding anilines with high yields. The catalytic activity and integrity of the catalyst remained almost unaffected for at least 5 cycles of reaction, which is due to the reformation of the fresh mineral at the end of each cycle. Of particular importance is the hydrogenation of the drug molecules “flutamide” and “nimesulide” at room temperature and pressure with the use of AB as the hydrogen source. The superiority of *in-situ* generation of Cu^0NPs compared to other Cu-based catalyst is that Cu^0NPs can be formed as fresh when needed, preventing any possible

aggregation or oxidation problem during reaction cycles or the storage of the catalyst. This work paves the way for the solution of common deactivation challenges of earth-abundant catalysts.

Experimental Section

Materials: All chemicals were purchased from commercial suppliers and used without further treatment: copper (II) sulfate pentahydrate ($\text{CuSO}_4 \cdot 5\text{H}_2\text{O}$, Sigma-Aldrich, 98%), sodium borohydride (NaBH_4 , Sigma-Aldrich, 99%) ammonia borane (NH_3BH_3 , Sigma-Aldrich, 90%), methanol (Fisher Chemical, $\geq 99.9\%$), nitrobenzene (Sigma-Aldrich, 99%), 1-chloro-4-nitrobenzene (Sigma-Aldrich, 99%), 1-fluoro-4-nitrobenzene (Sigma-Aldrich, 99%), 1-bromo-4-nitrobenzene (Sigma-Aldrich, 99%), 1,3-dinitrobenzene (Sigma-Aldrich, 97%), 3-nitropyridine (Sigma-Aldrich), aniline (Acros Organics, 99.8%), 4-chloroaniline (Alfa Aesar, 98%), 4-fluoroaniline (Sigma-Aldrich, 99%), 4-bromoaniline (Apollo Scientific), m-phenylenediamine (Sigma-Aldrich, 99%), 3-aminopyridine (Sigma-Aldrich, 99%), flutamide (Sigma-Aldrich), nimesulide (Sigma-Aldrich), deuterium oxide (Sigma-Aldrich), methanol- d_4 (Sigma-Aldrich).

Characterization: Powder X-ray diffraction (PXRD) data on all samples were collected on a Bruker D8 Advance diffractometer at ambient temperature using monochromated Cu $K\alpha$ radiation ($\lambda = 1.5418 \text{ \AA}$), with a 2θ step of 0.02° and a 2θ range of ~ 2 to 80° . The morphologies of our synthetic form of Jacquesdietrichite and *in-situ* generated Cu^0NPs were investigated by scanning electron microscopy (SEM) on the FEI Teneo SEM instrument and transmission electron microscopy (TEM) on the FEI Tecnai Spirit instrument. For SEM measurements, all samples were deposited on a carbon tape and coated with a 7-nm thick Iridium layer prior imaging. X-ray photoelectron spectroscopy (XPS) experiments were performed using PHI 5000 Versaprobe-II instrument from Physical Electronics. Samples were deposited on an insulating double sided, vacuum compatible, tape, and charge neutralization was applied during the XPS measurements. Auger electron spectroscopy (AES) was performed on a Kratos, Axis supra, equipped with a field emission electron gun operated at 10KeV, $\sim 5\text{nA}$. The UV-Vis absorbance spectra were obtained with a PerkinElmer UV-Vis Spectrometer. ^1H NMR analyses were performed on a Varian 400 MHz NMR spectrometer.

Catalyst preparation: For the formation of our synthetic form of Jacquesdietrichite, first 250 mg $\text{CuSO}_4 \cdot 5\text{H}_2\text{O}$ dissolved in 25 mL H_2O and 123 mg NaBH_4 dissolved in 25 mL H_2O were mixed together at room temperature for 30 minutes. The as-synthesized Cu NPs were washed with deionized water, then 20 mg of NPs were dispersed in AB/water solution (10 mg AB dissolved in 10 mL H_2O). The solution was exposed to open atmosphere and stirred gently overnight at room temperature under ambient conditions. The BO_2^- ions in the solution, Cu NPs derived from the Cu(II) salt, and the O_2 molecules in the air combined and formed the synthetic form of Jacquesdietrichite mineral ($\text{Cu}_2[(\text{BO})(\text{OH})_2](\text{OH})_3$). The blue solid was collected and washed with Millipore water and acetone several times, then dried under air at room temperature.

Hydrogenation of nitroarene compounds: The hydrogenation experiments were performed in a 25.0 mL Pyrex glass reactor, at room temperature under vigorous mixing. In a typical experiment, a molar ratio between the mineral, nitroarene and AB compounds (the molar ratio for the optimized conditions: mineral/nitroarene/AB = 0.086/0.172/1, exceptionally for nimesulide, the molar ratio: mineral/nimesulide/AB = 0.086/0.051/1) was determined. First, the nitroarene and mineral were suspended in the mixture of 9 mL methanol/Millipore water solution and the glass reactor was sealed with septum. Then, the suspension was sonicated, and purged with nitrogen for 20 minutes under gentle stirring to remove the dissolved oxygen. In a separate vial, 18 mg AB was dissolved in 1 mL of Millipore water and injected in the reaction solution, resulting in 10 mL of total reaction solution ($V_{\text{methanol}}:V_{\text{H}_2\text{O}} = 1:9$). A stirring speed of 750 rpm was employed during the reaction in order to eliminate any mass transfer limitation effects. When the reaction was complete, *in-situ* generated Cu^0 NPs were removed from the reaction solution by centrifugation and 50 μL of reaction product was extracted from the top of the supernatant. The extracted solution was further diluted by 200 times using methanol/water solution for UV-Vis analysis. Calibration curves were constructed by preparing methanol/water solutions of each commercial aniline compound at different concentrations, to determine the yields of reaction products. The purity of products was confirmed by ^1H NMR analysis by performing the same reactions in the mixture of methanol- $\text{d}_4/\text{D}_2\text{O}$ solutions. Some part of the reaction solution was extracted and used for the ^1H NMR analysis without further treatment. The yields for the reduced drugs were calculated using ^1H NMR analysis by adding THF as the internal standard. The reaction was performed using the optimized amount of catalyst and AB, and a known amount of reactant (0.1 mmol for flutamide and 0.03 mmol for nimesulide), in 10 mL of methanol- $\text{d}_4/\text{D}_2\text{O}$ solution. After the reaction is

complete, 10 μ L of THF was added and the solution was stirred for 15 minutes. Then, 1 mL of the reaction solution was extracted and ^1H NMR analysis was performed. The integration of the signal of the internal standard and product was made for the calculations of the product yield. While the integration of each peak for THF represents 4 hydrogens, the peak for the product was selected as it represents 1 hydrogen.

Acknowledgements

K.C.S. and T.N.N. thank Swiss National Science Foundation (SNF) for funding under the Ambizione Energy Grant n.PZENP2 166888. Authors thank Dr. Samantha L. Anderson for useful discussions.

Keywords: ammonia borane • metal nanoparticles • hydrogenation • heterogeneous catalysis • materials science

References

- [1] P.L. Hansen, J.B. Wagner, S. Helveg, J.R. Rostrup-Nielsen, B.S. Clausen, H. Topsøe, *Science* **2002**, *295*, 2053-2055.
- [2] L. Xu, H.-W. Liang, Y. Yang, S.-H. Yu, *Chem. Rev.* **2018**, *118*, 3209-3250.
- [3] J.A. Rodríguez, J. Evans, J. Graciani, J.-B. Park, P. Liu, J. Hrbek, J.F. Sanz, *J. Phys. Chem. C* **2009**, *113*, 7364-7370.
- [4] a) K. Yoshida, C. Gonzalez-Arellano, R. Luque, P.L. Gai, *Appl. Catal., A* **2010**, *379*, 38-44; b) R. Kaur, C. Giordano, M. Gradzielski, S.K. Mehta, *Chem. Asian J.* **2014**, *9*, 189-198; c) D. Formenti, F. Ferretti, F.K. Scharnagl, M. Beller, *Chem. Rev.* **2018**, *119*, 2611-2680.
- [5] B.J. Borah, D. Dutta, P.P. Saikia, N.C. Barua, D.K. Dutta, *Green Chem.* **2011**, *13*, 3453-3460.
- [6] J.H. Kim, Y.K. Chung, *Chem. Commun.* **2013**, *49*, 11101-11103.
- [7] X. Guo, C. Hao, G. Jin, H.Y. Zhu, X.Y. Guo, *Angew. Chem. Int. Ed.* **2014**, *53*, 1973-1977.
- [8] M.B. Gawande, A. Goswami, F.-X. Felpin, T. Asefa, X. Huang, R. Silva, X. Zou, R. Zboril, R.S. Varma, *Chem. Rev.* **2016**, *116*, 3722-3811.
- [9] a) D. Mott, J. Galkowski, L. Wang, J. Luo, C.-J. Zhong, *Langmuir* **2007**, *23*, 5740-5745; b) Y. Wang, A.V. Biradar, G. Wang, K.K. Sharma, C.T. Duncan, S. Rangan, T. Asefa, *Chem. Eur. J.* **2010**, *16*, 10735-10743; c) M. Jin, G. He, H. Zhang, J. Zeng, Z. Xie, Y. Xia, *Angew. Chem. Int. Ed.* **2011**, *50*, 10560-10564.

- [10] a) M.L. Kantam, V.S. Jaya, M.J. Lakshmi, B.R. Reddy, B. Choudary, S. Bhargava, *Catal. Commun.* **2007**, *8*, 1963-1968; b) P. Puthiaraj, W.-S. Ahn, *Catal. Sci. Technol.* **2016**, *6*, 1701-1709; c) M. Zahmakıran, F. Durap, S. Özkar, *Int. J. Hydrogen Energy* **2010**, *35*, 187-197.
- [11] a) M. Grouchko, A. Kamyshny, S. Magdassi, *J. Mater. Chem.* **2009**, *19*, 3057-3062; b) T. Yamauchi, Y. Tsukahara, T. Sakata, H. Mori, T. Yanagida, T. Kawai, Y. Wada, *Nanoscale* **2010**, *2*, 515-523; c) G. Zhou, M. Lu, Z. Yang, *Langmuir* **2006**, *22*, 5900-5903.
- [12] S. Campisi, M. Schiavoni, C. Chan-Thaw, A. Villa, *Catalysts* **2016**, *6*, 185.
- [13] X. Meng, L. Yang, N. Cao, C. Du, K. Hu, J. Su, W. Luo, G. Cheng, *ChemPlusChem* **2014**, *79*, 325-332.
- [14] A.R. Kampf, G. Favreau, *Eur. J. Mineral.* **2004**, *16*, 361-366.
- [15] F.P. Kinik, T.N. Nguyen, E. Oveisi, B. Valizadeh, F.M. Ebrahim, A. Gładysiak, M. Mensi, K.C. Stylianou, *J. Mater. Chem. A* **2019**, *7*, 23830-23837.
- [16] Q. Sun, N. Wang, T. Zhang, R. Bai, A. Mayoral, P. Zhang, Q. Zhang, O. Terasaki, J. Yu, *Angew. Chem. Int. Ed.* **2019**, *58*, 18570-18576.
- [17] K. Weissermel, H.-J. Arpe, *John Wiley & Sons* **2008**.
- [18] L. Petrov, K. Kumbilieva, N. Kirkov, *Appl. Catal.* **1990**, *59*, 31-43.
- [19] R.N. Brogden, S.P. Clissold, *Drugs* **1989**, *38*, 185-203.
- [20] a) Y.-s. Jian, C.-W. Chen, C.-A. Lin, H.-P. Yu, H.-Y. Lin, M.-Y. Liao, S.-H. Wu, Y.-F. Lin, P.-S. Lai, *Int. J. Nanomedicine* **2017**, *12*, 2315; b) T. Dey, P. Chatterjee, A. Bhattacharya, S. Pal, A.K. Mukherjee, *Cryst. Growth Des.* **2016**, *16*, 1442-1452; c) D. Formenti, F. Ferretti, C. Topf, A.-E. Surkus, M.-M. Pohl, J. Radnik, M. Schneider, K. Junge, M. Beller, F. Ragaini, *J. Catal.* **2017**, *351*, 79-89.
- [21] R.V. Jagadeesh, A.-E. Surkus, H. Junge, M.-M. Pohl, J. Radnik, J. Rabeah, H. Huan, V. Schünemann, A. Brückner, M. Beller, *Science* **2013**, *342*, 1073-1076.
- [22] S.A. May, *Journal of Flow Chemistry* **2017**, *7*, 137-145.
- [23] U. Sanyal, U. B. Demirci, B. R. Jagirdar, P. Miele, *ChemSusChem* **2011**, *4*, 1731-1739.
- [24] D. Tahir, S. Tougaard, *J. Phys. Condens. Matter* **2012**, *24*, 175002.
- [25] Y. Okazaki, K. Yamashita, H. Ishii, M. Sudo, M. Tsuchitani, *J. Appl. Toxicol.* **2003**, *23*, 315-322.
- [26] M. Telkar, J. Nadgeri, C. Rode, R. Chaudhari, *Appl. Catal. A* **2005**, *295*, 23-30.
- [27] D. Wei, H. Li, Y.-N. Li, J. Zhu, *Fluid Phase Equilib.* **2012**, *316*, 132-134.
- [28] M. M. Dell'Anna, S. Intini, G. Romanazzi, A. Rizzuti, C. Leonelli, F. Piccinni, P. Mastroilli, *J. Mol. Catal. A – Chem.* **2014**, *395*, 307-314.

- [29] C. Yu, J. Fu, M. Muzzio, T. Shen, D. Su, J. Zhu, S. Sun, *Chem. Mater.* **2017**, *29*, 1413-1418.
- [30] M. Madasu, C.-F. Hsia, S. Rej, M.H. Huang, *ACS Sustain. Chem. Eng.* **2018**, *6*, 11071-11077.
- [31] U. Sharma, P. Kumar, N. Kumar, V. Kumar, B. Singh, *Adv. Synth. Catal.* **2010**, *352*, 1834-1840.